

## Three-dimensional approximate local DtN boundary conditions for prolate spheroid boundaries

Hélène Barucq, Rabia Djellouli, Anne-Gaëlle Saint-Guirons

► **To cite this version:**

Hélène Barucq, Rabia Djellouli, Anne-Gaëlle Saint-Guirons. Three-dimensional approximate local DtN boundary conditions for prolate spheroid boundaries. *Journal of Computational and Applied Mathematics*, Elsevier, 2009, 10.1016/j.cam.2009.08.032 . inria-00338506

**HAL Id: inria-00338506**

**<https://hal.inria.fr/inria-00338506>**

Submitted on 13 Nov 2008

**HAL** is a multi-disciplinary open access archive for the deposit and dissemination of scientific research documents, whether they are published or not. The documents may come from teaching and research institutions in France or abroad, or from public or private research centers.

L'archive ouverte pluridisciplinaire **HAL**, est destinée au dépôt et à la diffusion de documents scientifiques de niveau recherche, publiés ou non, émanant des établissements d'enseignement et de recherche français ou étrangers, des laboratoires publics ou privés.

# Three-dimensional approximate *local* DtN boundary conditions for prolate spheroid boundaries

H. Barucq<sup>1,2</sup>, R.Djellouli<sup>3,1</sup>, A. Saint-Guirons<sup>2,1</sup>,

<sup>1</sup>*INRIA Futurs Research Center Team-Project Magique3D*

<sup>2</sup>*Laboratoire de Mathématiques Appliquées, CNRS UMR 5142, Université de Pau et des Pays de l'Adour, IPRA-Avenue de l'Université, 64013 Pau, France*

<sup>3</sup>*Department of Mathematics, California State University Northridge, CA 91330-8313, USA*

---

## Abstract

We propose a new class of approximate *local* DtN boundary conditions to be applied on prolate spheroid-shaped exterior boundaries when solving acoustic scattering problems by elongated obstacles. These conditions are : (a) exact for the first modes, (b) easy to implement and to parallelize, (c) compatible with the local structure of the computational finite element scheme, and (d) applicable to exterior ellipsoidal-shaped boundaries that are more suitable in terms of cost-effectiveness for surrounding elongated scatterers. We investigate analytically and numerically the effect of the frequency regime and the slenderness of the boundary on the accuracy of these conditions. We also compare their performance to the second order absorbing boundary condition (BGT2) designed by Bayliss, Gunzburger and Turkel when expressed in prolate spheroid coordinates. The analysis reveals that, in the low frequency regime, the new second order DtN condition (DtN2) retains a good level of accuracy *regardless* of the slenderness of the boundary. In addition, the DtN2 boundary condition outperforms the BGT2 condition. Such superiority is clearly noticeable for large eccentricity values.

*Key words:* Absorbing boundary conditions, prolate spheroidal coordinates, Dirichlet-to-Neumann operator, scattering problems

---

---

*Email address:* [helene.barucq@univ-pau.fr](mailto:helene.barucq@univ-pau.fr), [rabia.djellouli@csun.edu](mailto:rabia.djellouli@csun.edu), [anne-gaelle.saint-guirons@univ-pau.fr](mailto:anne-gaelle.saint-guirons@univ-pau.fr) (H. Barucq<sup>1,2</sup>, R.Djellouli<sup>3,1</sup>, A. Saint-Guirons<sup>2,1</sup>).

## 1 Introduction

Exterior Helmholtz problems are classical mathematical models for studying scattering problems arising in many applications such as sonar, radar, geophysical exploration, nondestructive testing, etc... Despite their simplicity, this class of problems is not completely solved particularly from a numerical point of view. For example, the computation of the solutions of these problems requires first to limit it to a finite domain. This is often achieved by surrounding the given scatterer(s) (or radiator) by an artificial boundary that is located at some distance (measured in multiples of wavelength of interest) from its surface. A so-called “nonreflecting” boundary condition is then prescribed on the artificial boundary to represent the “far-field” behavior of the scattered field. The challenge here is the development of a simple but reliable as well as cost-effective computational procedure for representing the far-field behavior of the scattered. The quest for such conditions is ongoing (see, e.g., the recent review by Turkel in the book [18]).

We propose in this work new three-dimensional approximate *local* DtN boundary conditions to be employed on prolate spheroid boundaries that are primary candidates for surrounding elongated scatterers. The idea for constructing such conditions is driven by several considerations chief among them the following two reasons. First, the widely-used second order absorbing boundary condition (BGT2) designed by Bayliss, Gunzburger and Turkel for spherical-shaped boundaries [4] performs poorly when it is expressed in elliptical coordinates and applied to prolate spheroid boundaries in the low frequency regime [14]. The accuracy deteriorates significantly for large eccentricity values of the boundaries as observed in [14]. The damping effect introduced to this condition [15] improves the performance for small eccentricity values. However, the modified BGT2 still performs poorly for eccentricity values larger than 0.6 in the (relatively) low frequency regime (see Figure 15 in [15]). Hence, there is a need for constructing local absorbing boundary conditions (ABC) that extend the range of satisfactory performance. Second, the three-dimensional approximate local DtN conditions designed for spherical-shaped boundaries [10] perform very well for low wavenumber values as reported in [11]. We recall that, in  $\mathbb{R}^3$ , the second-order DtN boundary condition and the BGT2 condition are identical [11]. Nevertheless, using these conditions on spherical-shaped exterior boundaries when solving scattering problems by elongated scatterer often leads to larger than needed computational domains, which hampers computational efficiency. This suggests that approximate local DtN boundary conditions designed for prolate spheroidal-shaped boundaries is an attractive alternative for improving the computational performance.

Given that, this work is devoted to the construction of theses conditions and to the assessment of their performance when employed on prolate spheroidal-

shaped boundaries for solving three-dimensional radiating and scattering problems. The idea of constructing three-dimensional approximate *local* DtN boundary conditions is not new. Indeed, as stated earlier, such conditions have been already derived for spherical-shaped boundaries [10] (see also reference [18] and references therein). The construction procedure adopted in [10] is based on the localization of the truncated global DtN boundary condition [12]. The key ingredient of this procedure is the trigonometric identities that express high order derivatives of sine and cosine functions. However, this property is not satisfied by the angular spheroidal wave functions [5]. Consequently, the procedure used in [10] is no longer applicable to the truncated global DtN boundary operator when expressed in elliptical coordinates [9,8]. Hence, the construction methodology we propose for deriving the class of approximate local DtN boundary conditions in prolate spheroidal coordinates can be viewed as an *inverse-type* approach. More specifically, we start from a Robin-type boundary condition with unknown coefficients. Unlike the case of spherical coordinates, these coefficients depend on the angles  $(\varphi, \theta)$  of the prolate spheroidal coordinates. Such dependence is necessary to preserve the symmetry and local nature of the resulting boundary conditions. Then, we require that the considered condition to be an exact representation of the first modes. Consequently, the coefficients are the unique solution of a linear algebraic system.

We assess mathematically and numerically the performance of the constructed approximate local DtN boundary conditions. More specifically, we analyze the effect of low wavenumber and the eccentricity on the performance of these conditions in the case of three-dimensional radiating and scattering problems. We adopt the on-surface radiation condition formulation (OSRC) [13] in order to perform *analytically* this investigation. We note that such formulation is *not* appropriate for high frequency regime as observed previously in [2]. The main interest in the following analyses is to evaluate the performance of the proposed approximate local DtN conditions at low wavenumber to see if relatively small computational domains can be employed in order to avoid excessive computational cost. The OSRC formulation must be viewed as an extreme case while an exterior ellipsoidal-shaped boundary surrounding an elongated scatterer would be less “demanding” on the boundary condition. The analysis herein shows that the constructed *second-order* local DtN condition retains a good level of accuracy in the low frequency regime for all eccentricity values of the elliptical-shaped boundaries. We must point out that we have also performed a similar investigation when these conditions are employed for solving exterior three-dimensional radiating problems. However, because of space limitation, we do not report in this paper on the results obtained in this case. These results can be found however in [16].

## 2 Preliminaries

Throughout this paper, we use the prolate spheroidal coordinates  $(\xi, \varphi, \theta)$  which are related to the Cartesian coordinates  $(x, y, z)$  by the following transformation:

$$x = b \sin \varphi \cos \theta, \quad y = b \sin \varphi \sin \theta, \quad z = a \cos \varphi \quad (1)$$

where  $\varphi \in [0, \pi)$ ,  $\theta \in [0, 2\pi)$ . The parameters  $a$  and  $b$  respectively represent the major and the minor axes and are given by:

$$a = f \cosh \xi, \quad b = f \sinh \xi \quad (2)$$

where  $\xi$  is a strictly positive real number and  $f$  is the interfocal distance and is defined by:

$$f = \sqrt{a^2 - b^2} \quad (3)$$

We also define the eccentricity  $e$  on a prolate spheroid at  $\xi = \xi_0$ , by:

$$e = \frac{1}{\cosh \xi_0} = \sqrt{1 - \frac{b^2}{a^2}} \quad (4)$$

The eccentricity  $e$  characterizes the slenderness of the surface. It satisfies  $0 < e < 1$ . Note that when  $e \rightarrow 0$ , the prolate spheroid degenerates into a sphere and when  $e \rightarrow 1$ , the spheroid degenerates into a line with length  $2f$  on the  $z$ -axis.

Furthermore, any incident plane wave  $u^{\text{inc}}$  can be expressed in this coordinate system as follows:

$$u^{\text{inc}} = e^{ikf \cosh \xi (\cos \varphi \cos \varphi_0 + \tanh \xi \sin \varphi \sin \varphi_0 \cos \theta)} \quad (5)$$

where the wavenumber  $k$  is a positive number and  $\varphi_0$  is the incident angle.

We consider in this work three-dimensional acoustic scattering problems by ellipsoidal-shaped scatterers. Such a restriction allows us however to adopt the OSRC formulation and set the ellipsoidal-shaped artificial boundary on the boundary of the obstacle. In addition, we assume, for simplicity, that the scatterers are *sound-soft*. Consequently, the acoustic scattered field  $u^{\text{scat}}$  solution of a sound-soft ellipsoidal-shaped scatterer can then be expressed in terms of spheroidal wave functions as follows [17]:

$$u^{\text{scat}} = -2 \sum_{m=0}^{\infty} \sum_{n=m}^{\infty} (2 - \delta_{0m}) A_{mn} i^n R_{mn}^{(3)}(kf, \cosh \xi) S_{mn}(kf, \cos \varphi) \cos m\theta \quad (6)$$

where

$$A_{mn} = \frac{R_{mn}^{(1)}(eka, e^{-1}) S_{mn}(eka, \cos \varphi_0)}{N_{mn} R_{mn}^{(3)}(eka, e^{-1})} \quad (7)$$

and  $N_{mn}$  represents the normalization factor of the angular spheroidal wave functions [5] and  $\delta_{0m}$  is the Kronecker delta symbol.

We recall that  $R_{mn}^{(j)}$  represents the spheroidal wave functions of the  $j^{\text{th}}$  type (see p. in Reference [5]),  $S_{mn}$  denotes the angular wave functions.

We recall that the  $mn$ th prolate spheroidal mode is given by [17]:

$$u_{mn} = R_{mn}^{(3)}(kf, \cosh \xi) S_{mn}(kf, \cos \varphi) \cos m\theta \quad (8)$$

### 3 Three-dimensional approximate local DtN boundary conditions in prolate spheroid coordinates

The three-dimensional first-order (DtN1) and second-order (DtN2) local Dirichlet-to-Neumann boundary conditions, defined on the ellipsoidal-shaped boundary  $\xi = \xi_0$ , are given by:

$$\text{DtN1} : \quad \frac{\partial u}{\partial \xi} = \frac{\sqrt{1-e^2}}{e} R_{00} u \quad (9)$$

$$\begin{aligned} \text{DtN2} : \quad \frac{\partial u}{\partial \xi} = \frac{\sqrt{1-e^2}}{(\lambda_{01} - \lambda_{00})e} & \left[ (\lambda_{01} R_{01} - \lambda_{00} R_{00} - (R_{00} - R_{01})(eka)^2 \cos^2 \varphi) u \right. \\ & \left. + (R_{00} - R_{01}) \Delta_{\Gamma} u \right] \end{aligned} \quad (10)$$

where  $\lambda_{mn}$  represents the spheroidal eigenvalues [5] and the coefficients  $R_{mn}$  depend on the radial spheroidal wave functions of the third kind  $R_{mn}^{(3)}$ , the wavenumber  $ka$ , and the eccentricity  $e$  as follows:

$$R_{mn} = \frac{R_{mn}^{(3)}(eka, e^{-1})}{R_{mn}^{(3)}(eka, e^{-1})} \quad (11)$$

and  $\Delta_{\Gamma}$  denotes the Laplace Beltrami operator, which reads in prolate spheroidal coordinates  $(\xi, \varphi, \theta)$  as:

$$\Delta_{\Gamma} = \frac{1}{\sin \varphi} \frac{\partial}{\partial \varphi} \left( \sin \varphi \frac{\partial}{\partial \varphi} \right) + \frac{1}{\sin^2 \varphi} \frac{\partial^2}{\partial \theta^2} \quad (12)$$

We are going to shortly describe the procedure used for constructing these two local approximate DtN boundary conditions. More details can be found in [3] and [16].

As stated earlier in the introduction, the construction methodology we propose for deriving the class of approximate local DtN boundary conditions in prolate spheroidal coordinates can be viewed as an *inverse-type* approach. More specifically, we start from a Robin-type boundary condition with unknown coefficients. Hence, in the case of DtN2 condition, we set:

$$\frac{\partial u}{\partial \xi} = A u + B (\Delta_{\Gamma} - (eka)^2 \cos^2 \varphi) u \quad (13)$$

where  $A$  and  $B$  are constant (independent of  $\varphi$ ) to be determined. Note that, unlike DtN2 boundary condition for the spherical-shaped boundaries, the coefficients of this condition depend on the angular variable  $\varphi$ . Such dependence is necessary for constructing a *symmetric* boundary condition since the angular spheroidal wave functions satisfied differential equation [5]. Then, we observe that all radiating modes  $u_{mn}$  given by Eq. (8) satisfy

$$\Delta_{\Gamma} u_{mn} = \left( -\lambda_{mn} + (eka)^2 \cos^2 \varphi \right) u_{mn} \quad (14)$$

Hence, in order to determine the constants  $A$  and  $B$ , we assume that, at  $\xi = \xi_0$ , we have:

$$\frac{\partial u_{mn}}{\partial \xi} = A u_{mn} + B \left( \Delta_{\Gamma} - (eka)^2 \cos^2 \varphi \right) u_{mn}; \quad m = 0 \quad \text{and} \quad n = 0, 1 \quad (15)$$

Then, using Eq. (14), it follows that  $(A, B)$  is the unique solution of the following  $2 \times 2$  linear system:

$$\begin{cases} A - B \lambda_{00} = \frac{\sqrt{1-e^2}}{e} R_{00} \\ A - B \lambda_{01} = \frac{\sqrt{1-e^2}}{e} R_{01} \end{cases} \quad (16)$$

where the coefficients  $R_{mn}$  are given by Eq. (11).

The DtN2 boundary condition given by Eq. (10) is a direct consequence of solving the system (16) and substituting the expressions of  $(A, B)$  into Eq. (13). In the simpler case of DtN1 condition, we follow the same procedure which leads to figure out the coefficient  $C$  such that:

$$\frac{\partial u_{00}}{\partial \xi} = C u_{00} \quad (17)$$

where  $u_{00}$  has been defined at Eq. (8). Then we get  $C = \frac{\sqrt{1-e^2}}{e} R_{00}$  and we obtain condition (9).

The following two remarks are noteworthy:

- First, the boundary conditions (9), (10) are called *local* DtN conditions because they result from a localization process of the truncated global DtN boundary operator defined in [9,8]. The local feature of these conditions is of a great interest from a numerical view point. Indeed, the incorporation of these conditions in any finite element code introduces only mass- and stiffness-type matrices defined on the exterior boundary. The coefficients  $\lambda_{mn}$  and  $R_{mn}$  can be computed once for all at the preprocessing level.
- Second, it must be pointed out that when  $e = 0$  (the prolate spheroid becomes a sphere), conditions (9) and (10) are identical to the three-dimensional *local* DtN conditions designed for spherical shaped boundaries (see Eqs. (12)-(13) in [11]). This property can be easily established using the asymptotic behavior of the radial spheroidal wave functions of the third kind  $R_{mn}^{(3)}$  and the prolate spheroidal eigenvalues  $\lambda_{mn}$ .

Moreover, the boundary conditions (9) and (10) satisfy, by construction, the following property that one can easily verify:

**Lemma 1** *The first-order DtN boundary condition (DtN1) given by (9) is an exact representation of the first mode  $u_{00}$  given by Eq.(8).*

*The second-order DtN boundary condition (DtN2) given by (10) is an exact representation of the first mode  $u_{00}$  and the second mode  $u_{01}$  given by Eq.(8).*

#### 4 Performance analysis

In the following, we assess analytically and numerically the performance of the approximate local DtN1 and DtN2 boundary conditions given by (9) and (10). More specifically, we analyze the effect of low wavenumber  $ka$  and the eccentricity  $e$  on the performance of DtN1 and DtN2 in the case of sound-soft scattering problems. We adopt the on-surface radiation condition formulation (OSRC) [13] in order to perform this investigation analytically. As in [11,14,15], we assess the performance of the ABCs DtN1 and DtN2 using the *specific impedance* introduced in [6,7] as a practical tool for measuring the efficiency of ABCs in the context of the OSRC formulation. This *non-dimensional* quantity measures the effect of the truncated medium in physical terms. It provides a convenient indicator of the performance of a given approximate representation. In the elliptical coordinate system, the specific impedance can be expressed as follows:

$$Z = \frac{i\sqrt{1-e^2}ka u^{\text{scat}}}{\frac{\partial}{\partial \xi} (u^{\text{scat}})|_{\xi=\xi_0}} \quad (18)$$



Therefore, the specific impedance  $Z^{\text{exact}}$  corresponding to the exact solution for three-dimensional sound-soft acoustic scattering problems can be computed analytically using  $u^{\text{scat}} = -u^{\text{inc}}$  (see Eq. (5)), and the Fourier series given by Eq. (6) to evaluate  $\frac{\partial}{\partial \xi}(u^{\text{scat}})|_{\xi=\xi_0}$  (see, for more details, [14–16]).

#### 4.1 Mathematical results

The following lemma states the expression of the approximate specific impedances on the boundary of a sound-soft ellipsoidal-shaped scatterer at  $\xi = \xi_0$ . These expressions can be easily derived from Eq. (18) by using  $u^{\text{scat}} = -u^{\text{inc}}$  (see Eq. (5)), along with substituting  $u = -u^{\text{inc}}$  into the DtN conditions (9) and (10).

**Lemma 2** *The approximate specific impedance ( $Z^{\text{DtN1}}$ ) corresponding to the first order DtN boundary condition (DtN1) is given by:*

$$Z^{\text{DtN1}} = \frac{ieka}{R_{00}} \quad (19)$$

*The approximate specific impedance ( $Z^{\text{DtN2}}$ ) corresponding to the second order DtN boundary condition (DtN2) is given by:*

$$Z^{\text{DtN2}} = \frac{\lambda_{01} - \lambda_{00}}{(\lambda_{01}R_{00} - \lambda_{00}R_{01}) \left( -2i\alpha ka - (ka)^2 \tau - (eka)^2 \cos \varphi \right)} \quad (20)$$

where

$$\alpha = \cos \varphi \cos \varphi_0 + \sqrt{1 - e^2} \sin \varphi \sin \varphi_0 \cos \theta, \quad \tau = \left( \frac{\partial \alpha}{\partial \varphi} \right)^2 + \frac{1}{\sin^2 \varphi} \left( \frac{\partial \alpha}{\partial \theta} \right)^2 \quad (21)$$

and  $R_{00}$  and  $R_{01}$  have been defined in Eq. (11).

**Remark 3** Note that when  $e = 0$ , that is the prolate spheroid degenerates to sphere, the approximate DtN specific impedances given by Eqs. (19) and (20) are identical to the ones obtained in the case of spherical-shaped scatterers for an incident angle  $\varphi_0 = 0$  (see Eq. (136) of Lemma 5.2.1 in [11]).

Now, we recall (see Eq. (91), p. 3655 in [14]), that the asymptotic behavior of the exact specific impedance  $Z^{\text{ex3}}$  of the scattered field on the surface of a prolate spheroid as  $ka \rightarrow 0$  is given by:

$$Z^{\text{ex3}} \sim (ka)^2 - ika \quad (22)$$

**Proposition 4.1** *The asymptotic behavior of the approximate specific impedance  $Z^{\text{DtN1}}$  as  $ka \rightarrow 0$  is given by:*

$$Z^{\text{DtN1}} \sim (ka)^2 - ika \quad (23)$$

*The asymptotic behavior of the approximate specific impedance  $Z^{\text{DtN2}}$  as  $ka \rightarrow 0$  is given by:*

$$Z^{\text{DtN2}} \sim (1 - \alpha)(ka)^2 - ika \quad (24)$$

where  $\alpha = \cos \varphi \cos \varphi_0 + \sqrt{1 - e^2} \sin \varphi \sin \varphi_0 \cos \theta$ .

**Proof of Proposition 4.1.** This proof is detailed in [3] and [16].

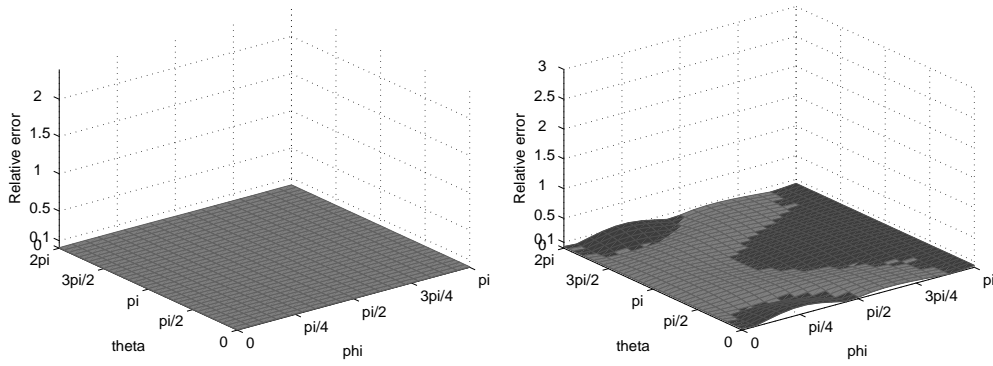
**Remark 4** First, we note that the asymptotic behavior of  $Z^{\text{DtN1}}$  is identical to the behavior of the exact specific impedance  $Z^{\text{ex3}}$  (see Eq. (22) and Eq. (23)). Second, Eq. (24) indicates that the asymptotic behavior of  $Z^{\text{DtN2}}$  depends on the eccentricity as well as on the observation angle  $\varphi$ . This dependence is comparable to the asymptotic behavior of the BGT2 approximate specific impedance (see Eq. (93), p. 3657 in [14]). Last, when  $e = 0$ , the asymptotic of both  $Z^{\text{DtN1}}$  and  $Z^{\text{DtN2}}$  are identical to the case of spheres (see Eq. (140) p. 47 in [11]).

#### 4.2 Illustrative numerical results

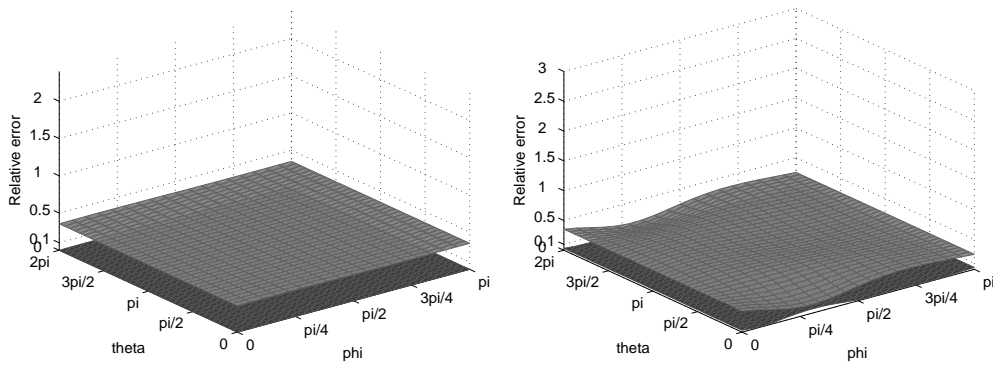
We have performed several experiments to investigate numerically the effect of the wavenumber and the slenderness of the boundary on the performance of the second-order DtN boundary condition DtN2 given by Eq. (10) when solving sound-soft scattering problems in the OSRC context. We have evaluated the relative error  $\frac{\|Z^{\text{ex3}} - Z^{\text{DtN2}}\|_2}{\|Z^{\text{ex3}}\|_2}$ . We have compared the results to the ones obtained with BGT2 condition (see Eq. (60) p. 3645 in [14]) when applied on prolate spheroid boundaries (see Figs. (22) to (33) in [14]). We report in here a sample of the results obtained for illustration. More numerical results can be found in [16]. Moreover, since the impedances in this case depend on  $\varphi \in [0, \pi)$  and  $\theta \in [0, 2\pi)$ , we have reported 3D plots of obtained results. These results have been obtained for three eccentricity values  $e = 0.1$  (corresponding to a prolate spheroid boundary very close to a sphere),  $e = 0.6$  (corresponding to a “regular” prolate spheroid boundary), and  $e = 0.9$  (corresponding to a very elongated prolate spheroid boundary), for two low wavenumber values  $ka = 0.1$  (on the left side),  $ka = 1$  (on the right side) and for an incident angle  $\varphi_0 = \frac{\pi}{4}$  (see Fig. (1)). One can observe that the DtN2 boundary condition delivers an excellent level of accuracy in the low frequency regime for all eccentricity values. Indeed, the results depicted in Fig. (1) indicate that the relative

error on the approximate DtN2 specific impedance is always below 2%, while the BGT2 accuracy deteriorates significantly for  $e \geq 0.6$  (the relative error is larger than 40%).

$e = 0.1$



$e = 0.6$



$e = 0.9$

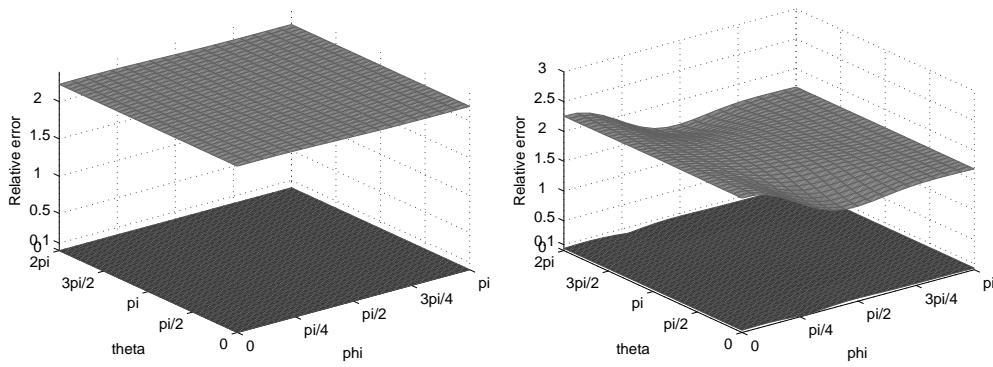


Fig. 1. Relative error of the absolute value of the specific impedance for the DtN2 (black) and the BGT2 (dark grey) for the incident angle  $\varphi_0 = \frac{\pi}{4}$ , and for  $ka = 0.1$  (left) and  $ka = 1$  (right).

## 5 Conclusion

We have designed a new class of approximate local ABCs to be applied on ellipsoidal-shaped exterior boundaries when solving acoustic scattering problems by elongated obstacles. These conditions are *exact* for the first modes, they are easy to implement and to parallelize, and they preserve the local structure of the computational finite element scheme. The analysis reveals that in the case of the radiator, DtN2 boundary conditions, by construction, outperforms the BGT2 conditions while performing similarly for small values of  $e$  and the DtN2 boundary condition outperforms BGT2 for lower single modes. However, for higher modes both conditions performs poorly. In the case of the scattering problem, the situation is different. Indeed, the BGT2 boundary conditions performs poorly for eccentricity values  $e \geq 0.6$  (the relative error  $\geq 40\%$ ), while the DtN2 boundary condition delivers an excellent level of accuracy (the relative error  $\leq 2\%$ ) in the low frequency regime for *all* eccentricity values. We are currently investigating analytically and numerically the effect of large values of the wavenumber on the accuracy of the DtN2 condition. We plan to report the results of this ongoing analysis in a separate note.

## Acknowledgments

The authors acknowledge the support by INRIA/CSUN Associate Team Program. Any opinions, findings, conclusions or recommendations expressed in this material are those of the authors and do not necessarily reflect the views of INRIA or CSUN.

## References

- [1] M. Abramovitz, I. Stegun, Handbook of Mathematical Functions with Formulas, Graphs and Mathematical Tables, Dover Publications, New York, 1972
- [2] X. Antoine, Fast approximate computation of a time-harmonic scattered field using the on-surface radiation condition method, IMA J. Appl. Math., 66(1):83–110, 2001
- [3] H. Barucq, R. Djellouli, A. Saint-Guirons, Construction and performance analysis of *local* DtN absorbing boundary conditions for exterior Helmholtz problems. Part II : Prolate spheroid boundaries, INRIA Research Report No 6395, (2007). Available online at: <http://hal.inria.fr/inria-00180475/fr/>

- [4] A. Bayliss, M. Gunzberger, and E. Turkel, Boundary conditions for the numerical solution of elliptic equations in exterior regions, *SIAM J. Appl. Math.*, 42 (2), pp. 430-451, 1982
- [5] C. Flammer, *Spheroidal Functions*, Stanford University Press, Stanford, CA, 1957
- [6] T. L. Geers, Doubly asymptotic approximations for transient motions of submerged structures, *J. Acoust. Soc. Am.*, 64 (5), pp. 1500-1508, 1978
- [7] T. L. Geers, Third-order doubly asymptotic approximations for computational acoustics, *J. Comput. Acoust.*, 8 (1), pp. 101-120, 2000
- [8] D. Givoli, Exact representations on artificial interfaces and applications in mechanics, *AMR*, 52(11):333-349, 1999
- [9] M. J. Grote, J. B. Keller, On nonreflecting boundary conditions, *J. Comput. Phys.*, 122, 2, 231-243, 1995
- [10] I. Harari and T. J. R. Hughes, Analysis of continuous formulations underlying the computation of time-harmonic acoustics in exterior domains, *Comput. Methods Appl. Mech. Engrg.*, 97(1):103-124, 1992
- [11] I. Harari, R. Djellouli, Analytical study of the effect of wave number on the performance of local absorbing boundary conditions for acoustic scattering, *Applied Numerical Mathematics*, 50, 15-47, 2004
- [12] J. B. Keller, D. Givoli, Exact nonreflecting boundary conditions, *J. Comput. Phys.*, 82 (1), 172-192, 1989
- [13] G. A. Kriegsmann, A. Taflove, and K. R. Umashankar, A new formulation of electromagnetic wave scattering using an on-surface radiation boundarycondition approach, *IEEE Trans. Antennas and Propagation* 35 (2), 153-161, 1987
- [14] R.C. Reiner, R. Djellouli, and I. Harari, The performance of local absorbing boundary conditions for acoustic scattering from elliptical shapes, *Comput. Methods Appl. Mech. Engrg.*, 195, 3622-3665, 2006
- [15] R.C. Reiner and R. Djellouli, Improvement of the performance of the BGT2 condition for low frequency acoustic scattering problems, *Journal of Wave Motion*, 43, pp. 406-424, 2006.
- [16] A. Saint-Guirons, Construction et analyse de conditions aux limites absorbantes pour des problèmes de propagation d'ondes, Ph.D. thesis, (In Preparation).
- [17] T. B. A. Senior, Scalar diffraction by a prolate spheroid at low frequencies, *Canad. J. Phys.* 38 (7) (1960) 1632-1641
- [18] E. Turkel, Iterative methods for the exterior Helmholtz equation including absorbing boundary conditions, In: *Computational Methods for Acoustics Problems*, F. Magoulès (ed.), Saxe-Coburg Publications (To Appear)